Journal of Solid State Chemistry 185 (2012) 238–244

Contents lists available at SciVerse ScienceDirect

Journal of Solid State Chemistry

journal homepage: www.elsevier.com/locate/jssc

Molecular dynamics simulations of solid state recrystallization I: Observation of grain growth in annealed iron nanoparticles

Jinfan Huang*, Lawrence S. Bartell

Department of Chemistry, University of Michigan, Ann Arbor, MI 48109, USA

ARTICLE INFO

Article history:
Received 25 April 2011
Received in revised form
31 August 2011
Accepted 14 September 2011
Available online 9 November 2011

Keywords:
Recrystallization
Grain growth
Grain boundary energies
Nucleation
Iron nanoparticles

ABSTRACT

Molecular dynamics simulations of solid state recrystallization and grain growth in iron nanoparticles containing 1436 atoms were carried out. During the period of relaxation of supercooled liquid drops and during thermal annealing of the solids they froze to, changes in disorder were followed by monitoring changes in energy and the migration of grain boundaries. All 27 polycrystalline nanoparticles, which were generated with different grain boundaries, were observed to recrystallize into single crystals during annealing. Larger grains consumed the smaller ones. In particular, two sets of solid particles, designated as A and B, each with two grains, were treated to generate 18 members of each set with different thermal histories. This provided small ensembles (of 18 members each) from which rates at which the larger grain engulfed the smaller one, could be determined. The rate was higher, the smaller the degree of misorientation between the grains, a result contrary to the general rule based on published experiments, but the reason was clear. Crystal A, which happened to have a somewhat lower angle of misorientation, also had a higher population of defects, as confirmed by its higher energy. Accordingly, its driving force to recrystallize was greater. Although the mechanism of recrystallization is commonly called nucleation, our results, which probe the system on an atomic scale, were not able to identify nuclei unequivocally. By contrast, our technique can and does reveal nuclei in the freezing of liquids and in transformations from one solid phase to another. An alternative rationale for a nucleation-like process in our results is proposed.

1. Introduction

The recrystallization of deformed bulk metals is important in technology and is a scientifically interesting process to understand, as well. Before going further it should be mentioned that the term recrystallization has been used in several different ways [1]. In the following, we adopt the common convention that recrystallization means the change in grain structure during annealing, which eliminates most of the dislocations through the migration of grain boundaries and the reduction of grain boundary area. In technology, this process introduces important changes in the properties of materials. In the treatment of metals plastically deformed by various techniques such as cold work or hot rolling, there is a stage in annealing at elevated temperatures known as recovery, which takes place before the recrystallization stage [2]. In recovery, stored internal strain energy is relieved by the partial removal of defects and dislocations. This process is a popular treatment of metallic materials [3]. It tends to restore the metal to its condition prior to the plastic deformation, a state in which the metal lattice still retains imperfections and grain boundaries. In the subsequent stage of recrystallization it is commonly said that the process consists of nucleation and growth [4], although an exact mechanistic definition of nucleation is elusive. It is supposed that nucleation in recrystallization involves small numbers of atoms in the grain boundaries. Therefore It is difficult to investigate experimentally and consequently, the presumed nucleation stage of recrystallization is poorly understood.

In the past two decades, research work on particles of nanometer size has become an active field in science and technology. Nanoparticles span the range between atoms on the one hand and bulk matter on the other. They link the microscopic world to the macroscopic world. They may have special properties distinguishing them from bulk matter. On the other hand, they may share many of the same properties such as phase changes, but because of their scale, they are accessible to techniques of measurement that bulk matter is not. Therefore nanoparticles may provide an avenue to study recrystallization on an atomic scale. In the past decade, we have studied nucleation in the crystallization of molten materials [5–9] and in phase transitions between different solid phases [10] using the technique of molecular dynamics (MD) on particles of nanometer size. In these studies as well as another [11,12], it was possible to recognize the nuclei, the entities giving the name to

* Corresponding author.
E-mail address: jinfanh@umich.edu (J. Huang).

0022-4596/$ - see front matter © 2011 Elsevier Inc. All rights reserved.
doi:10.1016/j.jssc.2011.09.015

nucleation, entities unavailable for observation, however, in studies of bulk matter. In the present work, nanoparticles of metal containing defects and grain boundaries were obtained not by the methods used to form bulk solids but by the rapid crystallization of supercooled liquid. One potential problem is that small clusters often freeze to icosahedra and not to the stable bulk phase. Fortunately, for some reason, our liquid iron clusters froze to the bcc structure of the bulk. In the present paper, we report our first MD study of solid state recrystallization during the thermal annealing of iron nanoparticles containing 1436 atoms. In a forthcoming paper we will report a study of recrystallization following the forging process.

2. Computational procedures

2.1. Generation of nanoparticles for kinetic studies

Disordered iron nanoparticles were formed by rapidly quenching molten droplets containing 1436 atoms. Molecular dynamics simulations of the behavior of selected examples were performed using an embedded-atom (EAM) potential [11,12] using 2 fs time steps in all of the simulations. The nanoparticles studied in the annealing process were generated by the following steps:

(1) *Generation of molten nanodroplets*: A spherical cluster containing 1436 iron atoms was formed by carving a particle with a radius of 1.9 nm, out of a body-centered cubic lattice of iron. The simulations began at constant temperature with 50,000 time steps in a bath at 200 K. A series of heating stages started at 300 K, with increments of 20°, each stage run at constant temperature for 50,000 time steps. The Fe_{1436} nanoparticle melted at about 1540 K but heating was continued to 1600 K to ensure complete melting.
(2) *Generation of molten nanodroplets with different thermal histories*: The molten nanodroplet obtained from process (1) was continuously heated at 1600 K to form 18 Fe_{1436} nanoparticles each with 50,000 more time steps than the previous one. This gave 18 melted Fe_{1436} particles with different thermal histories.
(3) *Generation of solid nanoparticles*: These 18 melted Fe_{1436} nanodroplets were quenched into heat baths at temperatures of 750, 800, 850, 900, 1000, and 1060 K, respectively, and kept in the baths for ~1200 ps. That yielded 108 quenching runs. Some of the runs produced crystals with two grains, and some with single crystals. The most deeply supercooled melts sometimes froze to solids with many grains.
(4) *Selection of polycrystalline nanoparticles for a study of recrystallization*: Particles in the set of solids generated as described in (3) were examined, and two particles consisting of two grains each were chosen for annealing runs. They came from the set quenched at 850 K about 25 ps after they were formed from the molten droplets. These two particles (which we hereafter designate as particles A and B) were then heated to 900 K, each retaining its grain structure during the process. Heating at 900 K was continued to generate 18 polycrystalline examples of particle A and 18 of particle B, each with different thermal histories, each example experiencing 2000 more time steps at 900 K than the previous one. An additional solid designated as particle C was also studied. When it was quenched, particle C froze to a single crystal.
(5) *Recrystallization studies*: The two sets of 18 nanoparticles generated in (4) were then annealed at constant temperature in a bath of 850 K. The number of time steps depended on the particle, as the simulation was discontinued after a single crystal was attained. In both of the small ensembles of A and B, some individuals annealed to single crystals quickly and some slowly. Therefore, from each ensemble could be derived a rate of transformation which, following nomenclature in the literature, we shall sometimes refer to as the nucleation rate.

2.2. Analysis of the recrystallization process

During the relaxation of the supercooled liquid and subsequent annealing of the solid, changes in structural and energetic properties could be monitored as a function of time. Initially after the quench, the molten droplets relaxed for awhile as seen in the decline in their energies with time. After freezing, strain energies due to crystalline imperfections and grain boundaries persisted until annealing ultimately removed them in the process of recrystallization.

A method of analysis alternative to energy is to monitor structural changes during the freezing and recrystallization. One such method was to check the linearity of the arrays of atoms corresponding to BCC cell edges disclosed dislocations. For an ideal BCC lattice, each atom has a coordination number of 8 and each atom in an array along cell edges is located at the crossing point of three orthogonal axes that connect the corners of the cells. For the sake of simplicity, we only consider the lines connecting an array of three atoms, with the central atom at the corner of a BCC cell. Accordingly, the central atom will be shared by at least two BCC cells. With this central atom as an origin, at the ends of the three orthogonal cell edges are six atoms appearing as sharp spots for a perfect crystal. For imperfectly packed nanoparticles these six spots may be defuse, as shown in Fig. 1 for an individual example from our Fe_{1436} nanoparticle at 400 K during the heating process. For a nanoparticle there will be many atoms with fewer than 8 such neighboring atoms. Returning to the array of three atoms along a cell edge: If this array is far from linear because of a surface or other imperfection, and if there are fewer than three nearly orthogonal lines crossing a cell corner, we will refer to these cases as having fewer than three "cross-overs" and use these in an analysis of dislocations and surfaces. In determining the number of "cross-overs" we considered neighboring atoms within the range of 2.76–2.96 Å lying along directions within 4° of perfect orthogonality.

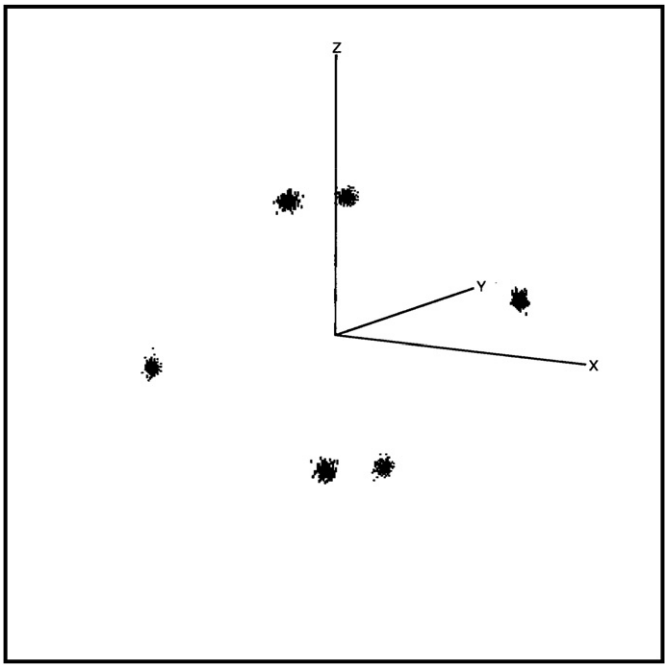

Fig. 1. Plot of the linearity orientation projection (LOP) for the crystalline solid at 400 K.

Table 1
Physical properties of bulk and nanoparticles of iron.

Properties	Value/expression	Reference
T_m (K)	1808	CRC handbook
T_b (K)	3134	CRC handbook
Δ_{Hfus} (kJ/mol)	14.9–16.2 (bulk)	CRC handbook
	4.6	For Fe_{1436} nanoparticle, this work
V_{ms} (solid) (m^3/mol)	$7.0\times10^{-6}+2.62\times10^{-10}$ T	For Fe_{1436} nanoparticle, this work
V_{ms} (solid) (m^3/mol)	$7.02\times10^{-6}+2.6\times10^{-10}$ T	Derived for bulk from CRC handbook
D (m^2/s)	$6.8322\times10^{-8}\exp(-5677/T)$	This work

2.3. Kinetics of formation of single crystals

If it is assumed that a nucleation mechanism governs recrystallization, then it might be expected that the fraction of particles in which a critical nucleus for recrystallization has not yet formed is characterized by a first-order rate law, which is by

$$N_n(t_n)/N_0 = e^{-JV_e}(t_n - t_0) \quad (1)$$

where t_0 is the time at which a grain boundary first begins to disappear, V_e is the volume of the grain boundary effective in nucleation (see a later discussion), N_0 is the number of total nucleation events studied in the ensemble, and t_n is the time at which the nth nucleation event N_n has taken place. Eq. (1) can be rewritten as

$$\ln[N_n(t_n)/N_0] = -JV_e((t_n - t_0) \quad (2)$$

where N_n (t_n) is taken to be [13]

$$N_n(t_n) = N_0 - n + 1 \quad (3)$$

From Eq. (2) is seen that the nucleation rate J for recrystallization can be obtained from the slope of the plot of $\ln[N_n(t_n)/N_0]$ vs. t_n. As will be seen, the MD results agree well with first order kinetics (Table 1).

3. Results

Fig. 2 plots the total energy as a function of time that the nanoparticles spend in the 850 K heat bath for three typical outcomes (A–C) of our 108 quenching runs. When the molten droplets were quenched into the heat bath of 850 K, the total energy dropped very sharply in the first few picoseconds after which the still molten, supercooled drops relaxed until they froze (at time t_0 in Eq. (1)). Particle A took ~750 ps to form a crystalline solid with two grains, this process of freezing corresponding to the second sharp drop on the energy curve. A third sharp drop in the energy curve began less than 70 ps later when the smaller grain began to be consumed by the larger grain. For nanodroplet B crystallization began after only ~100 ps in the heat bath and, again, a solid with two grains was formed. A third sharp drop on the energy curve began after the polycrystalline nanoparticle was annealed for ~600 ps in the heat bath. Particle C directly crystallized into a BCC single crystal, so that only two sharp drops in the total energy materialized. In all, 27 solids with at least two grains appeared and all recrystallized during the 108 quenching runs, with the remainder of the particles freezing directly into single crystals.

As mentioned above, there is only one sharp energy drop during the annealing process of polycrystalline solids A and B

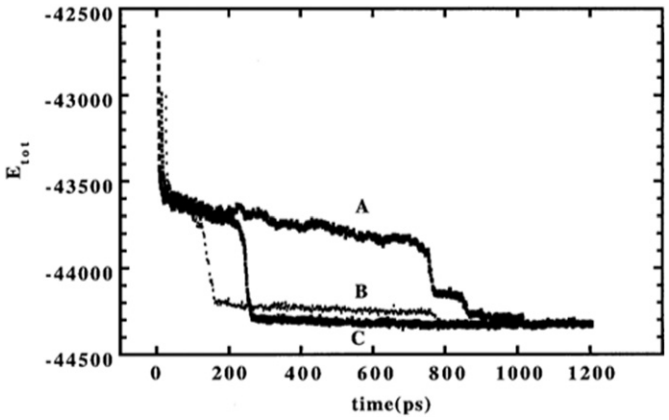

Fig. 2. Total energy per atom as a function of time during the quenching. Energy is in units of 1.3806×10^{-23} J/atom: (A) For particle A, which freezes into a solid with two grains, and then recrystallizes into a single crystal; (B) for particle B, which also freezes into a solid with two grains and then recrystallizes into a single crystal; and (C) for particle C, which directly freezes into single crystal.

generated in section II A (5). The onset of this sharp energy drop is taken to be tn for particle n in Eq. (1).

Images of nanoparticle A are given in Fig. 3. Fig. 3A shows that the two crystal grains remain in the particle 755 ps after the quench started and continue to persist for awhile. The bottom part of the image is a view from a direction perpendicular to 001(or 100/010) surface of a BCC lattice for the larger grain, a grain comprised of 9 layers. The upper part of the image shows the second grain with 6 layers of atoms viewed from a direction almost perpendicular to its 111 surface.

There is no conspicuous change in the image except for fluctuations, until the crystalline particle had been annealed at 850 K for about 65 ps (Fig. 3B–F). The image changed suddenly after 820 ps (Fig. 3G), and the entire reorganization ended within ~20 ps. The time at which this sudden change in image happened corresponds to the third sharp drop in energy in Fig. 2A.

Images of particle B are presented in Fig. 4. Fig. 4A shows the two grains in the particle that formed in the quenching. Both grains have about 8 layers of atoms at 150 ps from the start, but the one in the lower part of the image has more atoms in it. After the particle had been annealed at 850 K for another 200 ps, the lower grain acquired an extra layer of atoms (Fig. 4B). The slow growth of the lower grain during the next 300 ps can be seen in Fig. 4B and C. Between 650 ps and 750 ps (Fig. 4C–G) the lower grain grew quickly and the particle finally became a single crystal at ~750 ps (Fig. 4H). The beginning of the fast growth also corresponds to the third sharp drop on the energy curve in Fig. 2B. All of the 18 particles generated in II A (5) showed similar structural changes but with different time durations associated with each change.

Fig. 5 shows the number of cross lines that link the directions of three atoms at or adjacent to the corner of a BCC unit cell as a function of time for the two cases. The development with time is illustrated for cases A and B. What is learned from Fig. 5 is discussed in the next section.

4. Discussion

4.1. General considerations

Much of the prior research work on the recrystallization started from plastically deformed solids. As discussed in the Introduction, this involved recovery and recrystallization, which involved grain growth. The present incomplete understanding of

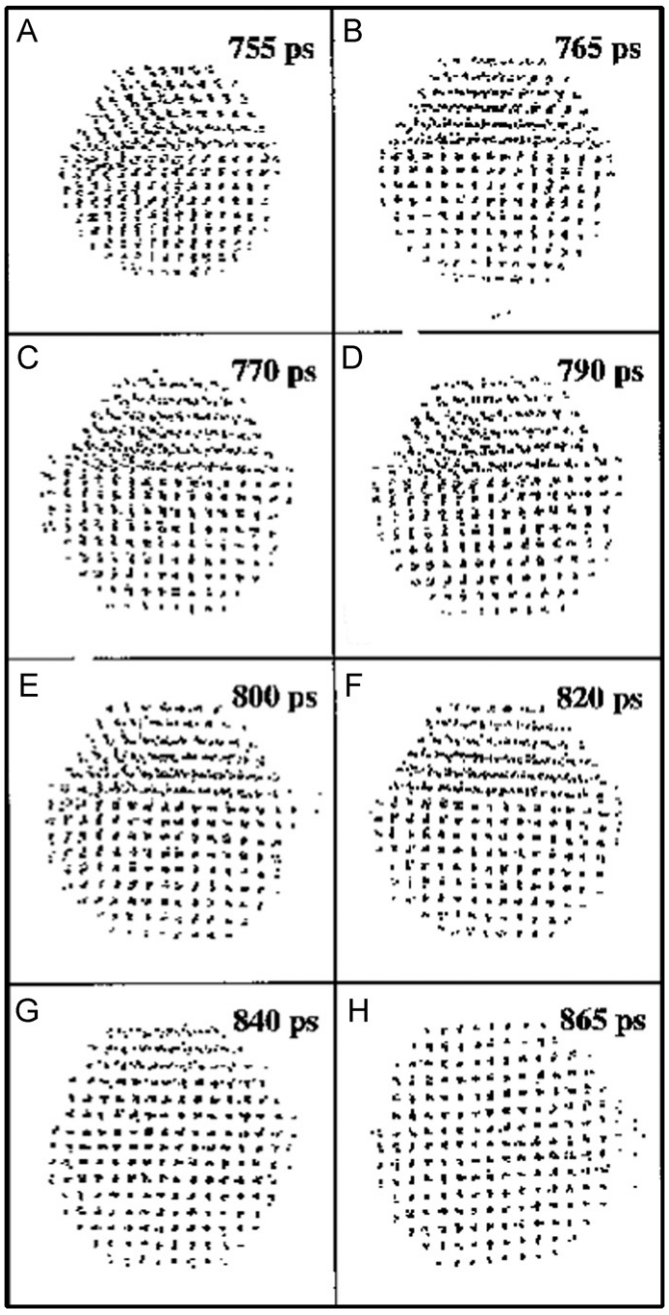

Fig. 3. Images of nanoparticle A at various times during the quenching run.

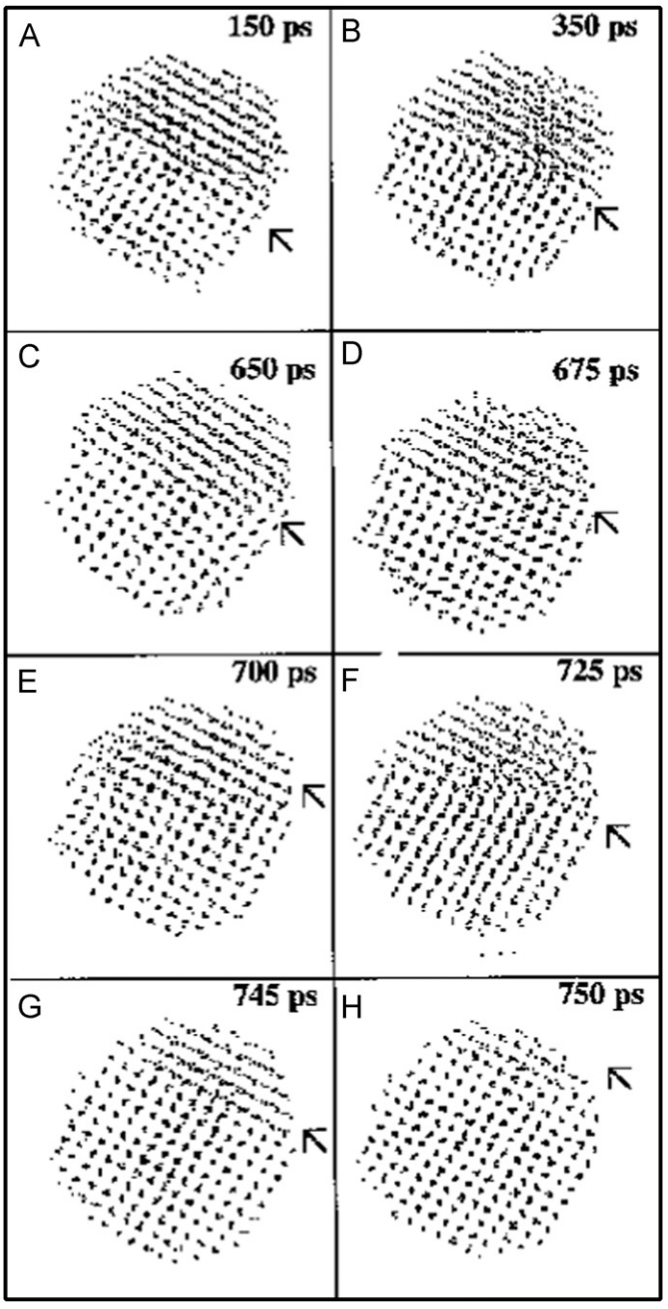

Fig. 4. Images of nanoparticle B at various times during the quenching run.

dislocations occurring during prior deformation of macroscopic solids, and the large-scale heterogeneities of deformation, which play important roles in recrystallization, impedes the construction of quantitative models of recrystallization. On the other hand, there is a great deal of information about the formation of grain boundaries during deformation, but no theories of annealing fully take this information into account. On annealing a cold-worked metal at an elevated temperature, defects or dislocations introduced during plastic deformation may be removed and the metal restored to its original state by the recovery process. In the annealing of the materials from casting or vapor deposition processes there may be a similar recovery process. In our MD simulations there is no deformation introduced analogous to that in the hot- or cold-working of metals. This seems to have eliminated the recovery process from consideration in our simulations, allowing us to focus on the process of recrystallization. Another advantage of MD simulations is that changes in a given grain boundary can be followed in atomic detail. Complications arising from heterogeneities of boundary misorientations and any interactions between multiple grains are avoided. This potentially allows a straightforward study of what has been considered the process of nucleation in the recrystallization of solids.

4.2. Strain energy and initiation of nucleation

Strain is the main driving force in recrystallization, and MD simulations provide a direct way to monitor strain by calculating the energy of the system. As shown in Fig. 2, particle A crystallized into two grains with more strain energy than particle B acquired on freezing. Nevertheless, particle B suffers more strain than particle C, which froze directly into a single crustal.. The slopes of the energy curves for annealing of particles A and B are

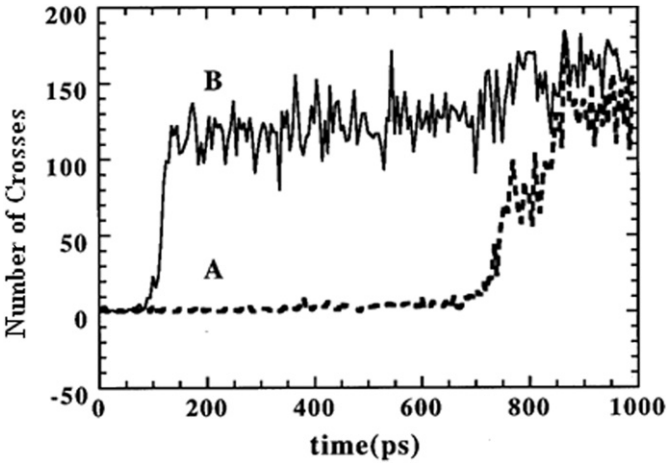

Fig. 5. Number of crosses that formed from two lines, which link at least three iron atoms at the corner of BCC cells; for particles A and B. See Sections 2, 2.2 for details.

similar to that of annealing of particle C. This suggests that the grain boundaries in A and B are major sources of the extra strain energy. Presumably, the time between the end of the second sharp drop and the beginning of the third sharp drop in the energies of A and B is the time to form what are presumed to be the critical nuclei for recrystallization.

4.3. Defects, dislocations, and microstructure changes

As depicted in Fig. 5, the dislocation change reflected by the changes in the total number of triplets of atoms aligned in nearly straight arrays is striking. The large change from supercooled liquid to polycrystalline solid suggests that this index is a useful diagnosis of disorder in small particles. The polycrystalline example A has more defects than that of solid particle B as inferred from the potential energies. The disappearance of dislocations in the short-range ordering in the two particles can be clearly seen in Fig. 5 showing when the freezing began.

4.4. Grain boundaries and grain boundary migration

Grain boundaries exist between crystalline grains and are characterized by the failure of the crystal planes of two grains to share the same orientation [2]. There are five degrees of freedom, two with the planes and three with the rotation angles. Once the boundary plane and the rotation axis are determined, then the smallest rotation angle around the rotation axis describes the misorientation between two crystal grains. As shown in Fig. 6A, the grain boundary between the two crystals in particle A exhibits an angle of misorientation of $\sim 31^\circ$ about the axis normal to the page, while for particle B the smallest rotation angle is larger, about 36° about the axis normal to the page as shown in Fig. 6B. These are large misorientations [2].

There are numerous idealized pictures of grain boundaries in many textbooks. In real life the grain boundary is not a thin, gently curved surface between two grains. As illustrated in Fig. 6A and B, there is no simple, sharply defined boundary between the two grains. In Figs. 7A and 8A all of the atoms belonging to the bottom grain are highlighted as dark dots based on the orientation of LOP. In Figs. 7 and 8, it is obvious that the grain boundaries are not flat planes but instead are convoluted regions in which some atoms have the orientation of one grain and some, the orientation of the other.

The migration of the grain boundary during recrystallization is shown in Figs. 7 and 8 for particles A and B using different

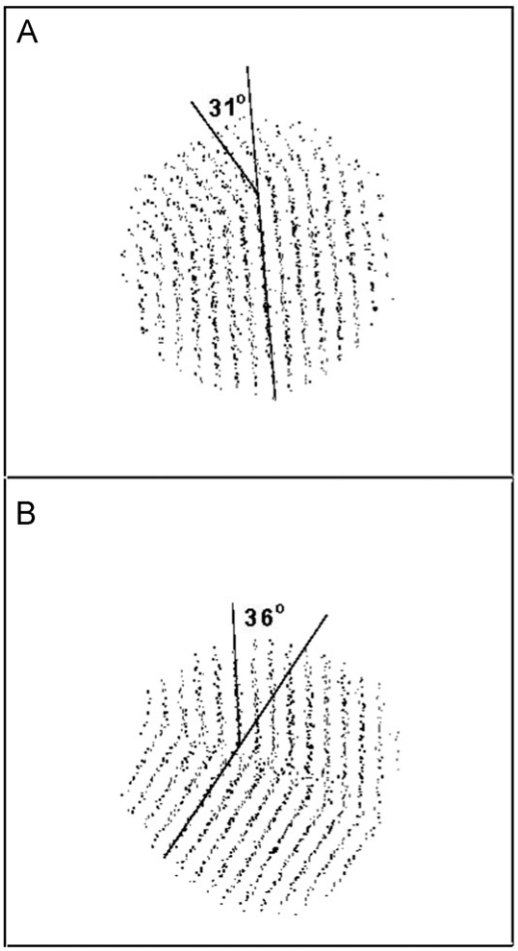

Fig. 6. Grain boundary misorientation angles, for particles A and B.

approaches. Fig. 7a–f shows snapshots of particle A at different times with all the atoms in the bottom grain identified by dark points while the atoms in the upper grains are depicted as light points. The migration of the boundary can be followed by comparing the snapshots at different times. Fig. 8A also highlights only the atoms in the bottom grain. Fig. 8b–f, instead, highlight those atoms growing from the larger grain into the upper grain in the time period of 100 ps for particle B. These atoms are the frontier of the growing grain. The outermost parts of these atoms near the second grain side is the grain boundary, which disappears in panel F. The fluctuation of the grain boundary before the concerted growth can be seen in both particles. One curious aspect in the behavior of the boundary in particle B is the motion of the grain boundary towards the smaller grain well before the third sharp drop in the total energy curve.

4.5. Nucleation rates in recrystallization

In the following discussion, we follow the widely expressed idea in the literature and assume for the time being that the activated process of coalescence of the two grains is one of nucleation. Figs. 9 and 10, then, plot the quantity $\ln[N_n(t_n)/N_0] \sim t_n$ of Eq. (2) for the small ensembles corresponding to particles A and B studied at 850 K. If, for sake of example, we arbitrarily take the volume of one layer of atoms between the two grains as the effective volume, the nucleation rates estimated from the slopes of these plots are $3.8(0.9) \times 10^{36}$ and $1.0(0.3) \times 10^{35}\ \mathrm{m^{-3}\,s^{-1}}$ for particles A and B, respectively. Had we chosen a different convention for the effective volume, it would have affected the absolute values of the rates but

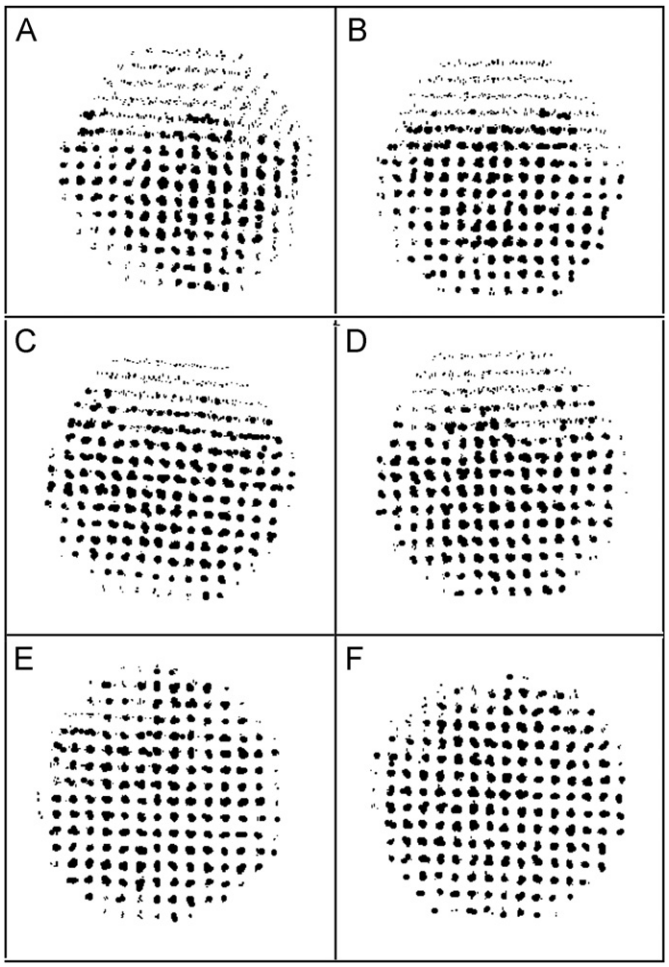

Fig. 7. Images showing grain boundary migration for particle A during the grain growth process. Darker spots represent the atoms from larger grain at times: (A) at 750 ps; (B) at 820 ps; (C) at 825 ps; (D) at 830 ps; (E) at 835 ps; and (F) at 840 ps.

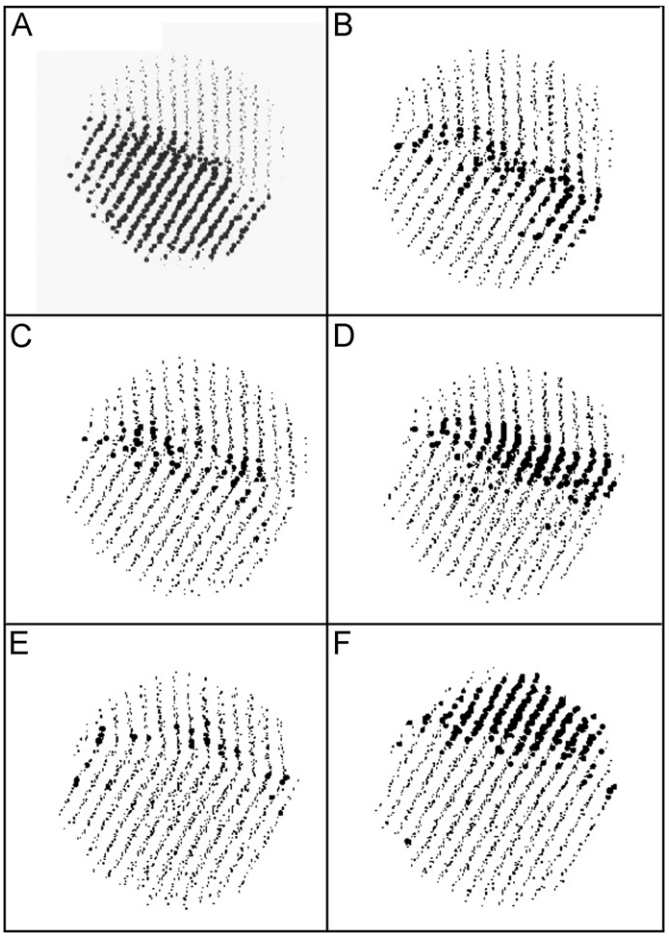

Fig. 8. Grain boundary migration for particle B during the grain growth process. The darker spots represent the atoms in the larger grain in (A) at time of 150 ps, while in (B–F), the darker spots represent the atoms migrating into the larger grain during the time periods as follows: (B) from 150 to 250 ps; (C) from 250 to 350 ps; (D) from 350 to 450 ps; (E) from 550 to 650 ps; and (F) from 650 to 750 ps.

would not have significantly altered the relative values in comparing rates for particles A and B. The difference in nucleation rates for these two different particles with different boundary properties is obviously large, more than one order of magnitude. What appears at first glance to be significant is that the higher nucleation rate corresponds to the polycrystal with the smaller grain boundary misorientation angle. This, however, contradicts the generally accepted and experimentally verified rule that the greater the angle of misfit, the greater the force to reorient and the faster the rate of reorientation [4]; present case, however, what overrides this rule is that particle A which, while freezing haphazardly, apparently suffers substantially more strain energy than particle B, as can be seen in Fig. 2. Why this happened is unknown but it clearly results in a driving force to relieve strain and hasten recrystallization.

Nucleation rates of recrystallization observed in this study are in the same range as was observed in our MD simulations of nucleation in the freezing of liquids and in the transformation of one sold phase into another [14]. It is recognized [3,15] that nucleation in recrystallization is fundamentally different from nucleation in transitions between different condensed phases where, in the latter case, the critical nucleus is a totally new embryo of the new phase that did not originally exist in the parent phase and is constructed through fluctuations atom by atom in the old phase to form a critical nucleus. By contrast, in recrystallization there is no nucleus of a new phase growing within the old crystalline phase because, except for the disorganized interface separating grains, there is only a single

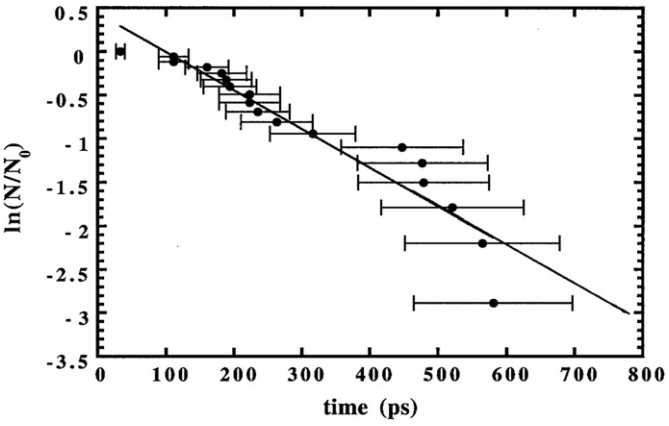

Fig. 9. Plot of $\ln[N_n(t)/N_0]$ vs. time for the ensemble of 18 runs for particle A.

phase. There is simply a greater tendency for a smaller grain than for a larger grain to dissolve into the interface between the grains and, in doing so, transfer matter to the larger grain.

Our MD simulations of recrystallization showed that the larger grain consumes the smaller grain resulting in a final single crystal which, naturally, has the same orientation as the initial larger grain. However, our simulation of particle B looks unusual in that

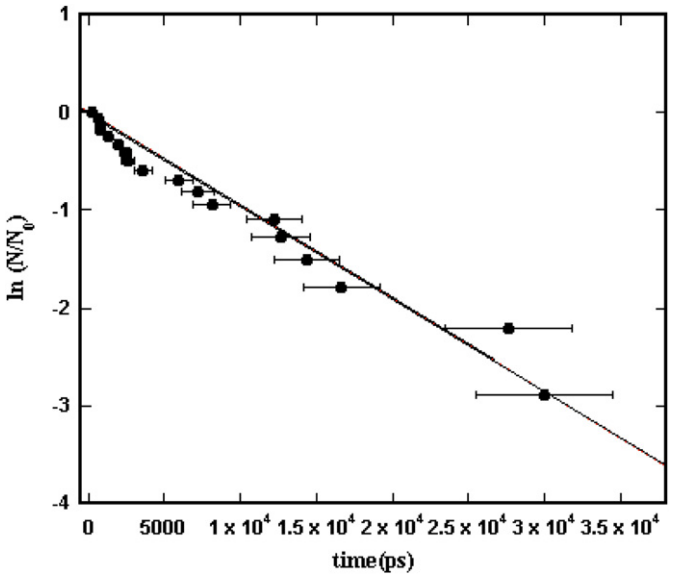

Fig. 10. Plot of $\ln[N_n(t)/N_0]$ vs. time for the ensemble of 18 runs for particle B.

the grain boundary begins to migrate toward the smaller grain well before the total energy drops sharply.

Although the rates or recrystallization derived in this study are of the same order of magnitude as the ones we found in our prior MD studies of nucleation rates in the freeing of liquids and in solid-state transitions [14]. This signifies very little other than that observations are adjusted until they can be followed on a reasonable computer timescale. Nevertheless, in our prior MD investigations of nucleation we could see and identify the nuclei involved. In the present MD simulations we were unable to identify entities which we could firmly establish as nuclei. We did find that the rate law corresponded to the law characteristic of homogeneous nucleation but that law is also characteristic of other kinds of activated processes. Therefore we cannot confirm the notion that anything like conventional nucleation is involved in recrystallization. What seems to be the case is that atoms in the smaller nucleus exhibit a greater tendency to escape into the grain boundary than do atoms in the larger grain, a situation analogous to the greater vapor pressure of small drops in comparison with large drops. Consequently, the larger grain has a greater tendency to acquire atoms from the grain boundary, and grow at the expense of the smaller grain. If this process can be supposed to correspond to a nucleation phenomenon, it may be because of the highly curved protuberances in the profiles of the surface of the grain boundary of the smaller grain, as seen in the images of Fig. 7. Therefore, these protuberances, or the cavities in the larger grain enhance the rate of escape of atoms from the smaller grain into the larger grain, so the formation of these protuberances may be crudely analogous to the formation of critical nuclei in conventional phase changes.

5. Concluding remarks

The present MD simulations of Fe_{1436} nanoparticles undergoing recrystallization provide several significant results. When a solid particle with two grains, one larger than the other, coalesces into a single grain, the larger grain grows at the expense of the smaller grain as expected from considerations of interfacial free energy. The rate at which recrystallization takes place is expected from prior experiments to be greater the greater the misorientation of the grains but, as observed in our simulations, the relief of the strain energy in newly formed grains can override effects of the magnitude of the misorientation. In the literature it is commonly said that in recrystallization, the transition takes place by nucleation. The kinetics of transformation we observed was first-order as expected from standard nucleation theory but that dos not prove that a conventional nucleation mechanism is involved. Unlike the situation in our prior MD simulations of phase transitions, we see no conspicuous nuclei and hence, cannot conclude that a mechanism similar to classical nucleation is involved. Certainly the process is activated, and it must take place by fluctuations, but these seem not to be localized into recognizable nuclei, unless we consider the protuberances of the smaller grain into the grain boundary as nuclei. Our incomplete diagnosis of what happens in studies of recrystallization in real systems motivates us to carry out further MD studies, including studies of cold-worked solids, and studies of particles of different sizes.

Acknowledgments

We are pleased to acknowledge helpful comments made by two referees.

References

[1] P.R. Rios, F. Siciliano Jr., H.R.Z. Sandim, R.L. Plaut, A.F. Padilha, Mater. Res. 8 (2005) 225–238.
[2] F.J. Humphreys, M. Hatherly, Recrystallization and Related Annealing Phenomena, 2nd Edition, Elsevier, Oxford, 2004.
[3] B. Hutchnson, et al., Thermomechenical Processing in Theory, Modeling and Practice, ASM International, Material Park, Ohio, 1997.
[4] R.D. Doherty, D.A. Hughes, F.J. Humphreys, J.J. Jonas, D. Juul Jensen, M.E. Kassner, W.E. King, T.R. McNelly, H.J. McQueen, A.D. Rollett, Mater. Sci. Eng. A238 (1997) 219–274.
[5] J. Huang, X. Zhu, L.S. Bartell, J. Phys. Chem. A102 (1998) 2708–2715.
[6] L.S. Bartell, J. Huang, J. Phys. Chem. A102 (1998) 8722–8726.
[7] H. Deng, J. Huang, J. Solid State Chem. 159 (2001) 10–18.
[8] X. Li, J. Huang, J. Solid State Chem. 176 (2003) 234–242.
[9] J. Huang, L.S. Bartell, J. Solid State Chem. 177 (2004) 1529–1534.
[10] Y.G. Chushak, L.S. Bartell, J. Phys. Chem. B103 (1999) 11196–11204.
[11] Y. Shibuta, T. Suzuki, J. Chem. Phys. 29 (2008) 144102.
[12] (a) M.S. Daw, S.M. Foiles, M.I. Baskes, Mater. Sci. Rep. 9 (1993) 251–310;
(b) Potential data for iron was from D. Farkas 〈http://www.ims.uccon.edu/centers/simul/pot/fefarkas.pot〉;
(c) XMD program. J. Rifkin jon.rifkin@uconn.edu at the University of Connecticut.
[13] Y. Chushak, P. Santikary, L.S. Bartell, J. Phys. Chem. 103 (1999) 56445636-103 (1999) 5644.
[14] J. Huang, unpublished result.
[15] R.D. Doherty, Recrystallization of Metallic Materials, in: F. Haessner (Ed.), Dr. Rieder Verlag, Berlin, 1978, p. 23.